Plasma Polymerized Multi-Layered Photonic Films

H. Jiang,[‡] W. E. Johnson,[†] J. T. Grant,[§] K. Eyink,[†] E. M. Johnson,[†] D. W. Tomlin,[||] and T. J. Bunning*,[†]

Air Force Research Laboratory, Materials and Manufacturing Directorate/MLP, Wright-Patterson Air Force Base, Ohio 45433-7702, Anteon Co., Dayton, Ohio 45431, Research Institute, University of Dayton, Dayton, Ohio 45469, and Technical Management Concepts, Inc., Beavercreek, Ohio 45434

Received June 10, 2002. Revised Manuscript Received November 4, 2002

A multilayer optical interference film has been developed using plasma-enhanced chemical vapor deposition (PECVD) of different organic precursor materials. A relatively large refractive index contrast for polymers (>0.2) is achieved by sequential plasma polymerization (PP) of octafluorocyclobutane (OFCB) and benzene. Gas-phase molecules of both precursors, excited by an argon plasma in a flowing afterglow reaction chamber, are deposited on a variety of substrates to form dense, pinhole-free, cross-linked polymer films. The PP-OFCB film yields a refractive index of 1.40, whereas PP-benzene exhibits a refractive index of 1.61 at 500 nm. We report here on the chemical (FTIR and XPS), optical (variable angle spectroscopic ellipsometry and UV−Vis spectrometry), and morphological (scanning electron microscopy) characterization of individually polymerized films of each component. These data are used to design a multilayer film with a notch at ∼1 μm. A ten-bilayer stack (alternating high and low refractive index) was fabricated by sequential deposition of high and low refractive index layers at approximately $^1/_4\lambda$ optical thickness. Optical spectra of the experimental stack exhibit a notch wavelength within several nanometers of the design wavelength indicating good thickness control.

Introduction

In the past four decades, the field of optical science and technology has been growing rapidly. Driven by the proliferation of the laser, optics has become integrated into a variety of fields including medicine, communication, transportation, aerospace, and the entertainment industry. A need to control the polarization, wavelength, amplitude, and direction of these light sources has stimulated the development of the optical component market. Today, the use of thin films to produce high-efficiency broadband mirrors, antireflection coatings, cold mirrors, hot mirrors, and narrow-notch filters is common.[1−4] The performance of these components is controlled by spatial control of the refractive index profiles. The bulk of these films are formed by depositing inorganic precursor materials, typically using various chemical vapor deposition (CVD) techniques. Inorganic materials have been exploited because of the large refractive index (RI) range available and the low absorption coefficients present. CVD-type processes suit these materials and also allow for the ability to make nonconventional refractive index profiles by simultaneous co-deposition of more than one component.

The use of polymers as linear optical components has been growing over the last several decades. Organic materials offer several advantages over inorganic materials including processability, compatibility, and economics. Simple one-dimensional stacks of processed polymer films were first reported nearly 2 decades ago,[5] and a high-performance version was reported more recently.[6] With the recent advent of photonic crystal research, a large flurry of activity has been centered on using various polymer-based platforms including block copolymers,[7,8] polymeric hydrogels,[9,10] and inorganic/organic hybrids[11,12] as optical band gap materials. The successful formation of one-dimensional multilayer interference films using organics is dictated by the refractive index contrast between the multilayer mate-

* To whom correspondence should be addressed. Phone: 937-255-3808. Fax: 937-255-1128. E-mail: timothy.bunning@wpafb.af.mil.
[†] Air Force Research Laboratory.
[‡] Anteon Co.
[§] University of Dayton.
[||] Technical Management Concepts, Inc.

(1) Françon, M. *Optical Interferometry*; Academic Press: New York, 1966.
(2) Tolansky, S. *An Introduction to Interferometry*; John Wiley & Sons: New York, 1973.
(3) Hariharan, P. *Optical Interferometry*; Academic Press: Sydney, Australia, 1985.
(4) Macleod, H. A. *Thin-Film Optical Filters*; Macmillan Publishing Company: New York, 1986.
(5) Alfery, T.; Gurnee, E. F.; Schrenk, W. J. *Polym. Eng. Sci.* **1986**, *9*, 400.
(6) Weber, M. F.; Stover, C. A.; Gilbert, L. R.; Nevitt, T. J.; Ouderkirk, A. J. *Science* **2000**, *287*, 2451.
(7) Edrington, A. C.; Urbas, A. M.; DeRege, P.; Chen, C. X.; Swager, T. M.; Hadjichristidis, N.; Xenidou, M.; Fetters, L. J.; Joannopoulos, J. D.; Fink, Y.; Thomas, E. L. *Adv. Mater.* **2001**, *13*, 421.
(8) Fink, Y.; Urbas, A. M.; Bawendi, M. G.; Joannopoulos, J. D.; Thomas, E. L. *J. Lightwave Technol.* **1999**, *17*, 1963.
(9) Xu, X.; Friedman, G.; Humfeld, K. D.; Majetich, S. A.; Asher, S. A. *Adv. Mat.* **2001**, *13*, 1681.
(10) Rundquist, P. A.; Photinos, P.; Jagannathan, S.; Asher, S. A. *J. Chem. Phys.* **1989**, *91*, 4932.
(11) Hart, S. D.; Maskaly, G. R.; Temelkuran, B.; Pridaux, P. H.; Joannopolous, J. D.; Fink, Y. *Science* **2002**, *296*, 510.
(12) Fink, Y.; Winn, J. N.; Fan, S.; Chen, C.; Michel, J.; Joannopoulos, J. D.; Thomas, E. L. *Science* **1998**, *282*, 1679.

10.1021/cm0206542 CCC: $25.00
Published on Web 12/17/2002

rials, control of the optical thickness ($n*t$), and the number of layers achievable. Limitations for organics include a small refractive index range and dimensional control of periodicity. Commercially available, easily processable, optical polymers have refractive indices in a narrow range between 1.45 and 1.6.[13] For visible multilayer stacks, this dictates physical thicknesses on the order of 75−100 nm. Thickness control in this regime is difficult; self-assembly processes typically occur on a much smaller length scale and therefore necessitate many steps to fabricate just one optical layer whereas standard spin-coating techniques are difficult to reproducibly control on such small length scales.

Approaches to achieve one-dimensional (narrow) band gap structures in the visible are driven by a need for the proper periodicity, high reflectivity (deep band-gap), and high transmission. High, narrow notch reflectivity is a function of many factors although the most important is the refractive index contrast.[4] Utilization of this contrast can occur in many different ways ranging from the classic ABAB stack to the more recently developed rugate (sinusoidally varying) profile.[14] The advantage of the latter type structure is increased transmission (elimination of higher-order harmonics) and better overall control of notch depth and width. Deposition techniques to allow inhomogeneous, continually varying refractive index profiles must allow co-deposition of both high and low RI compounds enabling a continuous grade of the film's RI.

The methodology for large scale production of organic coatings with controlled, periodic, and continuous variation (nonstep) in refractive index is still lacking. The use of plasma-enhanced chemical vapor deposition (PECVD) techniques offers the promise of dense cross-linked films with continuously varying refractive indices. Plasma polymerization of organic compounds is well-known and many studies have been reported.[15−17] Reacting an organic precursor in the gas phase with a plasma is a dry deposition technique suitable for automation which can be run at room temperature. Compared to conventional wet (solution) techniques, it generates very little waste and allows polymers to be formed from nonconventional precursors including aromatic heterocycles such as thiophene and furan.[18,19] Manipulation of the PECVD processing parameters allows for fine-tuning of the chemistry as well as the thickness. The ability to co-deposit two precursors simultaneously to get an average refractive index somewhere between the starting materials gives rise to the potential of continuously varying the refractive index profile in an organic film. In addition, PECVD is amenable to deposition on substrates with complicated geometries.

In the work presented here, both benzene and octafluorocyclobutane (OFCB) are used as precursor materials and are reacted in the flowing afterglow of an argon plasma.[18] Thin plasma-polymerized (PP) films of both compounds (PP-benzene and PP-OFCB) are investigated with X-ray photoelectron spectroscopy, Fourier transform infrared spectroscopy, scanning electron and optical microscopy, and variable angle spectroscopic ellipsometry. The rates of deposition and refractive indices were determined. This information was used to design and fabricate a multilayer stack using PP-benzene as the high refractive index material and PP-OFCB as the low refractive index compound. Optical spectroscopy measurements indicate good agreement with the theoretical notch as computed using the measured thicknesses (from scanning electron microscopy) and refractive index and absorption coefficients measured from ellipsometry. The structure of the stack is explored using SEM, and the optical properties are investigated using optical spectroscopy. This work indicates that PECVD can be used to fabricate complex photonic structures using nonconventional organic precursors.

Experimental Procedures

Optical grade benzene liquid was used as the high refractive index precursor; it was supplied by Aldrich Co. and had a purity of over 99%. Octafluorocyclobutane (OFCB), a compressed gas with purity of 99% supplied by TCI Co., was chosen as the low refractive index precursor. Both precursor materials were directly used in our experiments without any additional purification. Figure 1 shows a schematic of the PECVD reactor; the detailed description of the setup was published elsewhere.[18] Argon (50−200 cm^3/min, 99.999%), used as the noble gas for generating a plasma, flows into a 10-cm diam. reactor at 0.5−1 Torr vacuum through a capacitively coupled radio frequency (RF, 13.56 MHz) discharge of 5 to 30 W power. The plasma density is controlled to approximately 10^8 cm^{-3} in the afterglow region. The precursor gas/vapor is added 20 cm downstream from the plasma generation zone. The substrate is located about 1−3 cm further downstream from the precursor inlet. The distance between the substrates and the inlet of precursor materials can be changed as the requirements of the resulting films change. Precursor flow rates of 0.5 and 1.125 cm^3/min were utilized for the benzene and OFCB films, respectively. Thin films of each material were deposited on either silica wafers, glass, or IR transparent salt plates. A Sycon STM-100 thickness/rate monitor was used in preliminary measurements of film deposition rates. A Tencor P-10 surface profiler with a diamond stylus was used to perform profilometry. An average scan rate of 100 μm/s was used with a sampling rate of 200 points/second resulting in a spatial resolution of 0.5 μm/point.

Functional groups present in the plasma-polymerized films were identified through Fourier transform infrared (FTIR) analysis. Plasma-polymerized films were deposited directly onto potassium bromide (KBr) disks in the reaction chamber for subsequent analysis. FTIR analysis was performed on a Perkin-Elmer Spectrum 2000 FT-IR spectrometer in the transmission mode. A range of 400 to 4000 cm^{-1} was scanned 128 times in 1 cm^{-1} increments and averaged. X-ray photoelectron spectroscopy (XPS) was performed on a Surface Science Instruments' M-Probe spectrometer equipped with a monochromatic Al Kα X-ray source for photoelectron production with an energy of 1486.6 eV. Samples were deposited on silicon wafers and were mounted on an aluminum holder for analysis. The pressure in the chamber during analysis was between 2 and 4 × 10^{-8} Torr. The overall surface composition for each sample was determined using survey scans taken between 0 and 1000 eV binding energy. The chemistry of individual elements was examined by acquiring data at appropriate energy regions using the unscanned spectrometer mode. The spectrometer energy resolution was 1.5 eV for all

(13) Mark, J. E. *Physical Properties of Polymers Handbook*; American Institute of Physics: Woodbury, New York, 1996.
(14) Johnson, W. E.; Crane, R. L. *SPIE Proc.* **1993**, *2046*, 88.
(15) Yasuda, H. *Plasma Polymerization*; Academic Press: New York, 1985.
(16) Denes, F. *Trends Polym. Sci.* **1997**, *5*, 23.
(17) Shi, F. *Surf. Coatings Technol.* **1996**, *82*, 1.
(18) Haaland, P.; Targove, J. *Appl. Phys. Lett.* **1992**, *61*, 34.
(19) Haaland, P.; Ibrani, S.; Jiang, H. *Appl. Phys. Lett.* **1994**, *64*, 1629.

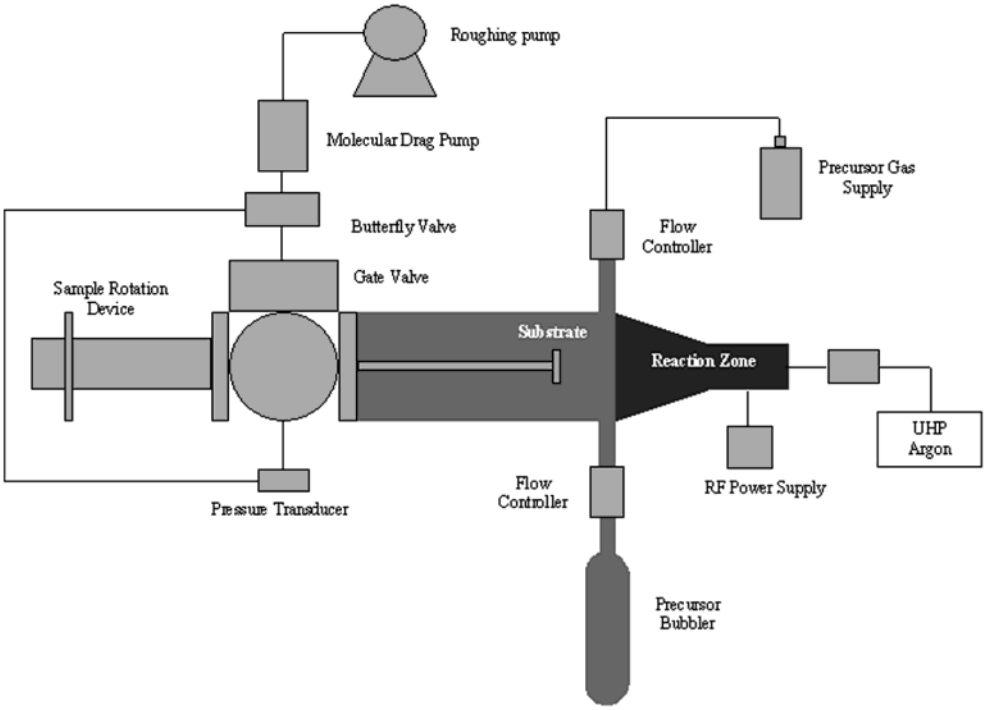

Figure 1. Schematic of plasma-enhanced chemical vapor deposition apparatus. Note the inlet of either precursor gas is after the reaction zone ensuring only interaction with metastable argon ions in the flowing afterglow region.

data; the spectrometer covered an energy range of approximately 20 eV in the unscanned mode. The analysis area on the samples was approximately 400 × 1000 μm.

Ellipsometry was used to determine both the optical properties and the thickness of the plasma-polymerized films. A Woollam variable-angle spectroscopic ellipsometer system including a VB-200 ellipsometer control module and a CVI Instruments DigiKrom 242 monochromator with a 75-W xenon light source was utilized. All data analysis was performed using Windows version 3.352 WVASE32 software. The reflected polarization states were acquired over the range of 300−900 nm at 1-nm intervals and at angles of incidence equal to 53°, 55°, and 57°. The dispersion in the refractive index (Cauchy model) for the each different polymer film was determined from the polarization data obtained from two plasma polymerized samples with different thicknesses on a Si(001) substrate.

A Hitachi S-900 low-voltage/high-resolution (LVHR) scanning electron microscope (SEM) was used to image the plasma polymer films. Plasma polymer films were deposited on silicon wafers and coated with 1−2 nm of tungsten using a VCR Group, Inc. (now South Bay Technologies) dual ion beam sputter coater, to eliminate sample charging and to enhance edge contrast.

Results and Discussion

A flowing afterglow technique,[18] utilized in this work, limits the interaction of the gas-phase precursor material with metastable argon species to form reactive species. This is possible because the ions and excited states formed in the plasma decay very rapidly, leaving metastable noble gas atoms in the afterglow region. The electronic energy of the argon metastable, about 11.5 eV, is sufficiently high to break most organic bonds.[16] Previous work by our group has demonstrated this technique can be used to form plasma-polymerized (PP) films from a variety of organic precursors including thiophene, furan, alkylsilanes, and cyclofluoro-compounds, without dissociative ionization.[19,20] These films have an amorphous structure, a smooth surface, are pinhole free, and are highly resistant to chemical attack.

The PECVD product of precursor benzene, PP-benzene, looks smooth and pale yellow to the unaided eye. It is insoluble in benzene, acetone, methanol, and dimethyl sulfoxide after immersion for more than 6 months. The FT-IR spectra of liquid benzene and PP-benzene (polyphenylene) film are given in Figure 2 a and b, respectively. The peaks in the 3000−3100 cm^{-1} region such as 3034 and 3089 cm^{-1} (Figure 2a) and 3024 and 3056 cm^{-1} (Figure 2b) correspond to aromatic C−H stretching.[21−23] The band at about 1035 cm^{-1} in the spectra corresponds to the C−H in-plane deformation of the benzene ring.[23] The peak at 1477 cm^{-1} in the benzene spectrum, corresponding to C═C ring stretching in $-C_6H_5$, splits into the 1494 and 1599 cm^{-1} bands upon plasma polymerization, indicating C═C conjugated and nonconjugated stretching caused by substitutions on the phenyl rings or ring opening upon plasma polymerization.[21,22,24] Many weak bands at around 700−900 cm^{-1} are vibrations consistent with a mixture of *m*-, *p*-, and *o*-linked rings in the polymer.[23,25,26] It is interesting to note in the PP-benzene spectrum, the aliphatic C−H stretching modes at 2800−3000 cm^{-1}, at 2860 cm^{-1} due to methyl, and at 2922 cm^{-1} due to methylene groups. Also, the band at 1451 cm^{-1} denotes the C−H bending in CH_2 and CH_3. In addition, there is

(20) Haaland, P.; Jiang, H. *ACS Polym. Prepr.* **1993**, *34*, 675.
(21) Tibbit, J. M. *J. Macromol. Sci. Chem.* **1976**, *A10*, 1623.
(22) Tanaka, K. *J. Appl. Phys.* **1991**, *70*, 5653.
(23) Durrant, S. F.; Mota, R. P.; de Moraes, M. A. B. *Thin Solid Films* **1992**, *220*, 295.
(24) Silverstein, R. M.; Webster, F. X. *Spectrometric Identification of Organic Compounds*; John Wiley and Sons: New York, 1998.
(25) Jesch, K.; Blear, J. E.; Kronick, P. L. *J. Polym. Sci.* **1966**, *4*, 1487.
(26) Seeger, M.; Gritter, R. J.; Tibbitt, J. M.; Shen, M.; Bell, A. T. *J. Polym. Sci., Polym. Chem. Ed.* **1977**, *15*, 1403.

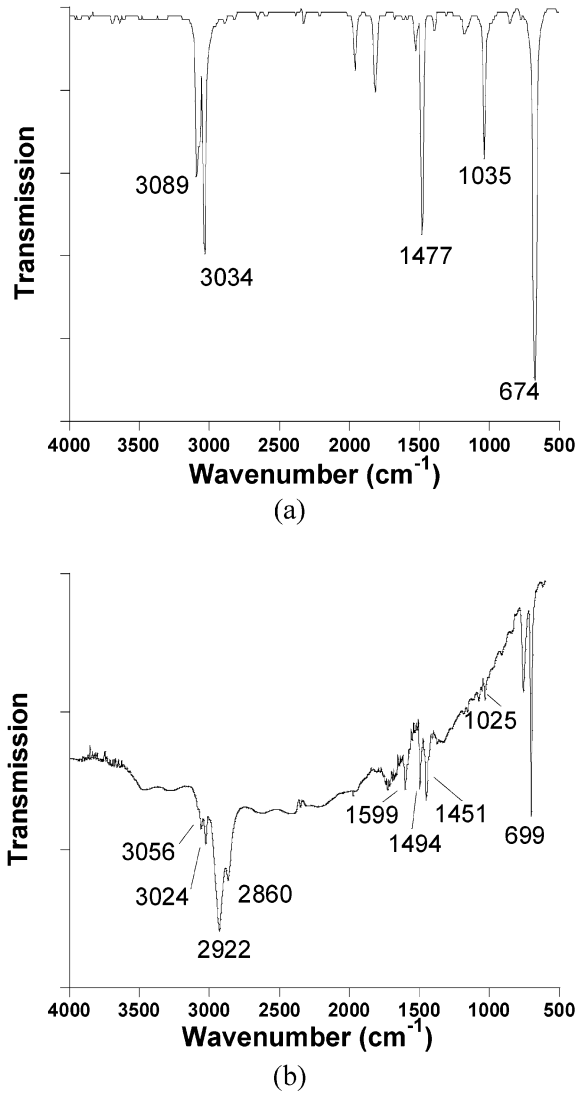

Figure 2. FT-IR spectra of pure liquid benzene (a) and plasma-polymerized benzene (b) on salt plate window.

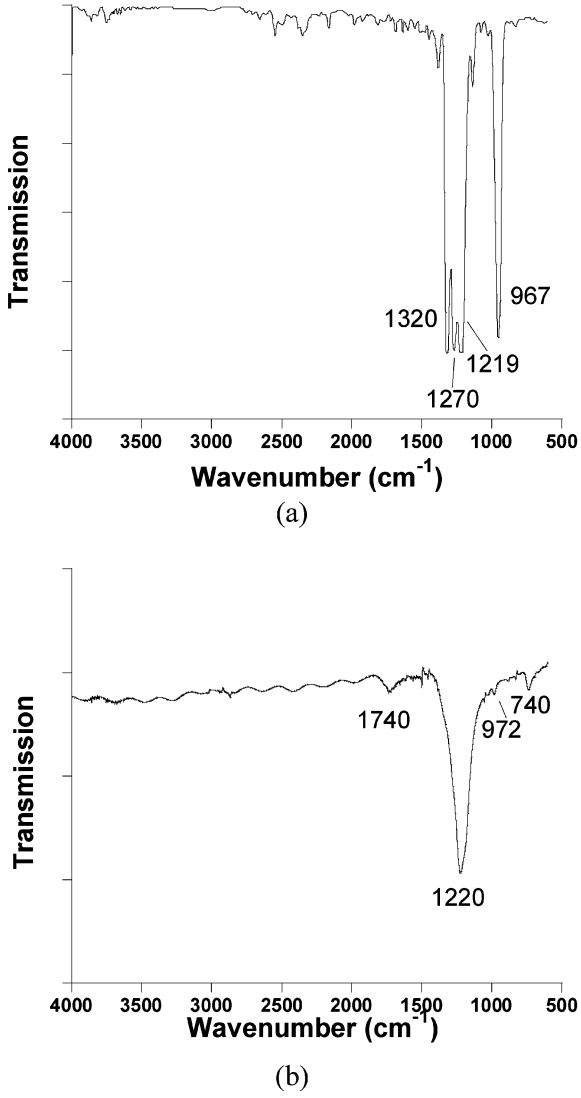

Figure 3. FT-IR spectra of pure octafluorocyclobutane (OFCB) (a) and plasma-polymerized OFCB (b) on salt plate window.

a small broad peak at 1600−1700 cm^{-1} due to the C═O stretch mode of carbonyl groups. These results suggest that a small fraction of benzene rings are retained after the PP reaction. The PP-benzene film is a highly cross-linked structure with both remnants of the six-membered aromatic ring and newly formed aliphatic structures formed by the plasma reaction. This film is different from the PP-benzene films produced directly in the plasma zone, as reported by previous authors.[23,24,27] In the latter, virtually all of the phenyl rings were destroyed during the plasma reaction so that the highly cross-linked structure had no, or only minimal, ring retention.[23,24,27]

Figure 3a and b show the FT-IR spectra of OFCB and PP-OFCB films, respectively. In the FT-IR spectrum of OFCB, the band at 967 cm^{-1} is caused by symmetric ring stretching of C_4F_8 molecules,[28] but in the PP-OFCB spectrum, the corresponding peak is essentially nonexistent. This means that the original ring structure of OFCB precursor is almost entirely destroyed during plasma processing. The bands at 1320 and 1270 cm^{-1} in the OFCB spectrum are due to asymmetric CF_2 stretches, whereas the band at 1219 cm^{-1} results from symmetric CF_2 stretching.[28] The corresponding peaks in the spectrum of PP-OFCB fall in a comparatively broad band at the region of 1100 to 1400 cm^{-1}, which is due to a convolution of CF_x (x = 1,2, or 3) stretching modes. The individual CF_x peaks located within this broad convoluted band are difficult to assign unambiguously.[29−31] Two small broad peaks located at 740 and 1740 cm^{-1} can also be seen in the PP-OFCB spectrum. The former is caused by the vibrations from amorphous fluoro-materials,[29,30,32] CF−CF_3 vibration, and zone center CF_2 system stretching,[29,30] which implies a traditional polymer chain structure.[29] The latter is due to the vibrations of ═C═CF_2, −C═CF_2, and −CF═CF_2 groups,[29,30] which signifies the existence of cross-linking structure in the film.[29] In addition, there is a small peak at 972 cm^{-1}, assigned as the vibration

(27) Han, L.; Timmons, R. B. *Chem. Mat.* **1998**, *10*, 1422.
(28) Shirafuju, T.; Miyazaki, Y.; Hayashi, Y.; Nishino, S. *Plasmas Polym.* **1999**, *4*, 57.
(29) Mackie, N. M.; Dalleska, N. F.; Castner, D. G.; Fisher, E. R. *Chem. Mater.* **1997**, *9*, 349.
(30) Ningel, K. P.; Theirich, D.; Engeman, J. *Surf. Coating Technol.* **1998**, *98*, 1142.
(31) Hynes, A. M.; Shenton, M. J. *Macromolecules* **1996**, *29*, 4220.
(32) Doucoure, A.; Guizard, C. *J. Membr. Sci.* **1996**, *117*, 143.

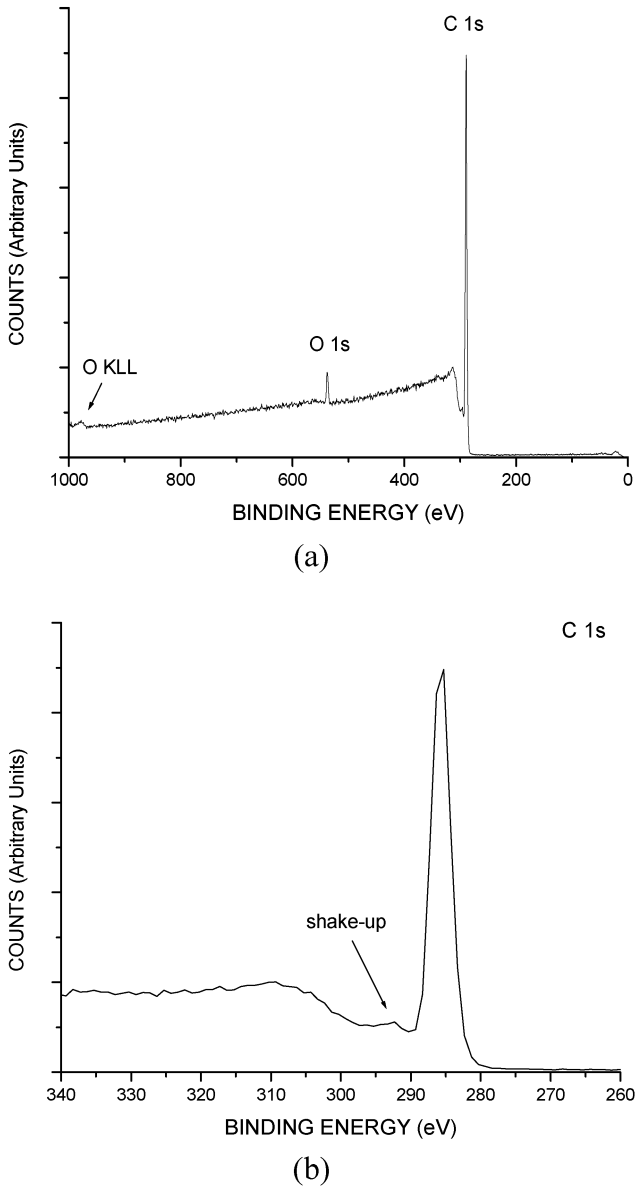

Figure 4. XPS survey scan from a PP-benzene film (a) and C 1s XPS scan showing the presence of the shake-up peak (b).

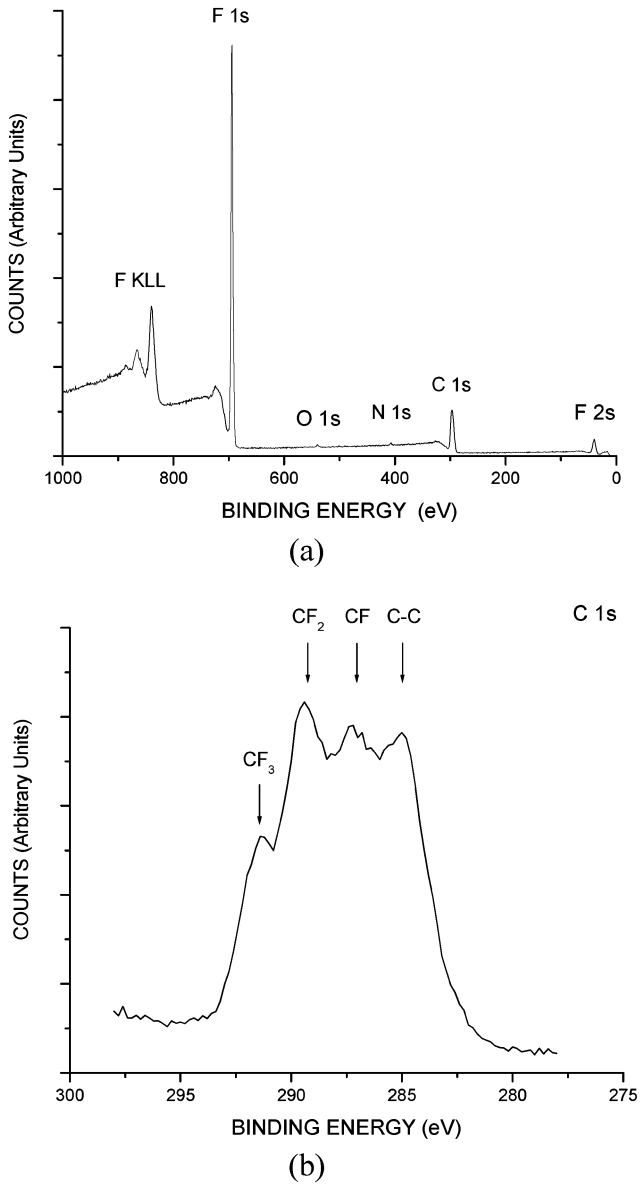

Figure 5. XPS survey scan from a PP-OFCB film (a) and C 1s XPS scan from a PP-OFCB film (b).

of CF_3.[29,30] These results indicate clearly that the PP-OFCB film contains both cross-linked and linear fluorinated polymers and oligomers, and that several different CF_x structural groups exist in the film.

The survey XPS spectrum from a PP-benzene film is shown in Figure 4a. The oxygen content of this film is 3 at. %. Of particular interest is the small feature about 7 eV to the high binding energy side of the C 1s peak. This is a shake-up peak due to unsaturated carbon bonds, and it is shown more clearly in Figure 4b. Even though this peak appears to be small, it is indicative of a high degree of unsaturated carbon in the PP-benzene film.[33] This result is consistent with the FT-IR results, which showed that a small percentage of the benzene rings were retained during the PP reaction.

An XPS spectrum from PP-OFCB is shown in Figure 5a. Besides the expected peaks from C and F, O and N were also detected but each had concentrations of only about 0.7 at. %. The F/C atomic ratio in the film is about 1.8, slightly less than the value of 2 for the precursor, C_4F_8. During plasma polymerization, the fluorine chemistry changed dramatically, as can be seen from the C 1s spectrum shown in Figure 5b. There are at least four peaks in this spectrum, and they correspond to CF_3, CF_2, CF, and CC bonds.[33] The CF_2 and CF bonds are of similar concentrations, and they are about double that of CF_3. The fluorine concentration required to satisfy the identification of the three carbon peaks associated with the indicated numbers of fluorine atoms agrees very closely with the measured fluorine concentration. The CC peak appears somewhat broader and has an intensity of about 1.5 times that of the CF_2 or CF peaks. The FT-IR results showed that the original ring structure of the OFCB was almost entirely destroyed during plasma processing, and that several different CF_x structural groups are present in the film. The XPS results show conclusively that this is indeed the case.

(33) Beamson, G.; Briggs, D. *High-Resolution XPS of Organic Polymers - The Scienta ESCA300 Database*; John Wiley & Sons: Chichester, UK, 1992.

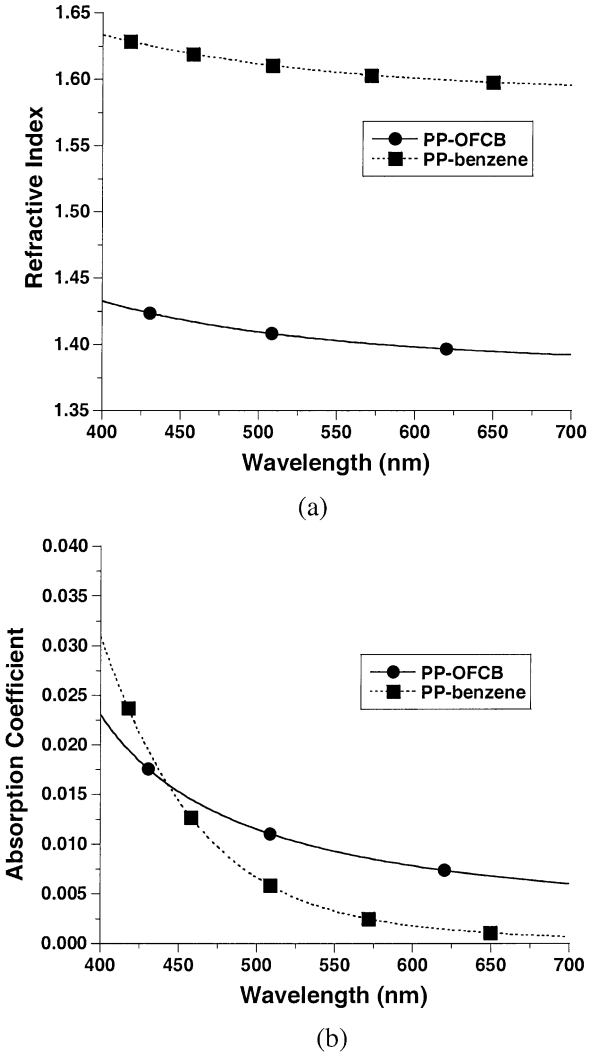

Figure 6. Refractive index (a) and absorption coefficient (b) dispersion curves from 400 to 700 nm for both PP-benzene and PP-OFCB.

The optical properties of both polymerized compounds obtained using ellipsometry are shown in Figures 6a and b. A large difference in refractive index between the two compounds is immediately observed. At 500 nm, the PP-benzene had a refractive index of 1.62 whereas PP-OFCB exhibited a RI of 1.40. The solid PP-benzene film's RI is considerably higher than that of pure, liquid benzene which exhibits a RI of 1.5. Substantial dispersion is present for both compounds as the RI reduces substantially as the wavelength is red-shifted across the visible spectra. Above 700 nm, little change occurs for either compound. The RI's of PP-benzene films deposited on silicon wafers and quartz disks were 1.63 and 1.62 respectively at 500 nm indicating a lack of significant substrate dependence. The experimentally determined value for PP-OFCB of 1.40 agrees well with the value of 1.375 ± 0.025 previously reported.[30] Such a low RI can be found in other fluorinated polymer materials but the number of materials with a RI < 1.4 are few and the number which are amenable to processing are fewer still. The PP-OFCB film has a refractive index very close to that of MgF_2, the inorganic material typically used for antireflection applications in the visible portion of the optical spectrum. These PP-OFCB films provide an alternative low index film when an inorganic AR coating is not compatible with the substrate. The RI contrast (~0.2) is high for these two different organic compounds.

The absorption coefficient data from the ellipsometer are shown in Figure 6b. A small, but measurable, value characterizes both plasma polymerized compounds. These values also show considerable dispersion with wavelength. The magnitude is largest in the blue and quickly diminishes as the wavelength is red-shifted. Surprisingly, the PP-OFCB films showed a larger value in the red part of the spectrum. This may be caused by residual free radicals or different oligomers in the films, or both. PP-benzene films' large value in the blue and the red shift in the spectrum are expected because of delocalization of electrons along more than one phenyl ring. These results are consistent with the FT-IR and XPS results discussed above.

Parameters were adjusted to ensure deposition rates were amenable to depositing multilayer films on an appropriate time scale. The determined rates were 21 nm/min for the PP-benzene film and 9 nm/min for the PP-OFCB film. Figure 7 shows both the surface and cross-sectional morphology as investigated by scanning electron microscopy. Dense films with little interior structure are exhibited. This is consistent with previous literature reporting use of this reactor setup.[18] No evidence of a columnar-like morphology, typically seen in thicker films, is observed at such thickness. The surfaces of the samples were very smooth. In fact, to provide contrast, artificial scratches in the films were made and then imaged. Probe microscopy results (not presented) indicated RMS roughness on the order of 1−2 nm over very large areas (mm^2). The thickness uniformity extended over several cm in lateral dimension.

The large RI contrast between the materials can be utilized to fabricate various photonic elements. Multilayer interference filters can be based on a series of transparent (nonabsorbing) layers (each a quarter wave in thickness) of different RIs.

The light reflected within the high-index layers does not undergo any phase change upon reflection, but the light reflected within the low-index layers will undergo a 180° phase shift upon reflection. As a result, all of the beams emerging at the upper surface of the optical stack are in phase and will interfere constructively. Therefore, it is possible to achieve high reflectance by forming alternative layers of transparent films with high and low refractive indices on a (transparent) substrate. The effective reflectance for an even number bilayer assembly can therefore be increased with the maximum reflectance obtained for a dielectric quarter wave stack given by

$$R_{\max} = \left[\frac{1 - \left(\frac{n_H}{n_L}\right)^{2p} n_s}{1 + \left(\frac{n_H}{n_L}\right)^{2p} n_s}\right]^2 \quad (1)$$

where n_H is the high refractive index, n_L is the low refractive index, and p is the total number of bilayers in the stack. Note, these equations all assume no absorption.

Using a design wavelength of 1 μm, a 10-bilayer stack was designed using the refractive indices measured from ellipsometry and deposition rates measured from ex-

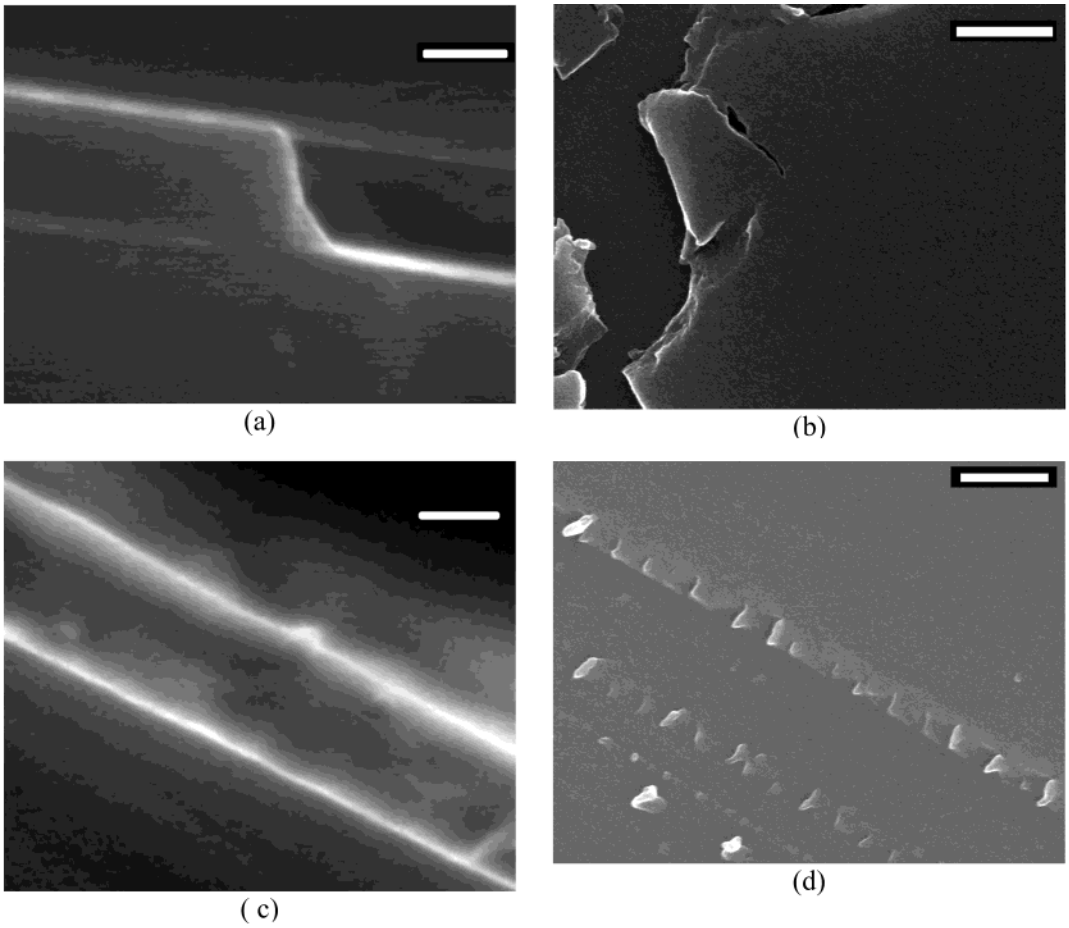

Figure 7. Scanning electron micrographs of the fractured edge (a) and surface (b) from a PP-benzene film, and of a fractured edge (c) and surface of a PP-OFCB film. Scale bars correspond to 150 nm (a and c) and 500 nm (b and d). Surfaces in (b) and (d) were intentionally scratched to allow focusing.

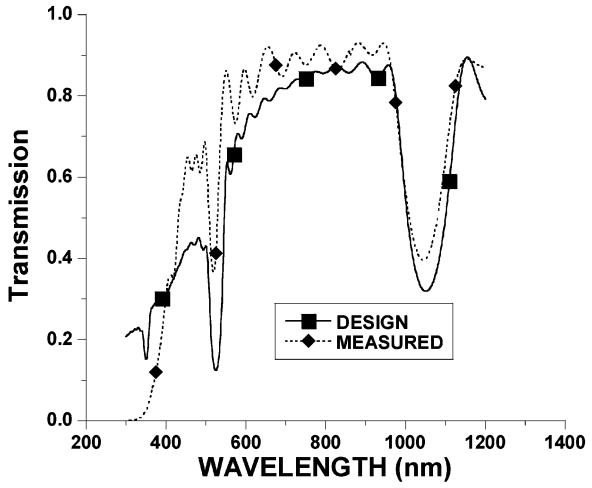

Figure 8. Experimental and calculated spectra of 10-bilayer stack fabricated using PECVD.

periment. The thicknesses of the individual layers were calculated from the QW condition and each layer was subsequently deposited on quartz. The optical spectrum of the multilayer stack is shown in Figure 8 along with a design spectrum (TFCalc software package (Software Spectra, Inc.)). Figure 9 shows SEM micrographs of the cross-section of the 10-bilayer stack (fractured in liquid nitrogen). The individual layers are dense and good adhesion is apparent. The wavelength of extinction matches the design wavelength indicating good control of the optical thickness. In an ideal QW stack, the even order harmonics should not appear; however, in the case of materials with slight absorption, they do appear. The ellipsometry results of the individual components indicate that a small finite absorption is present and thus we observe harmonics. Their appearance is also indicative of good agreement with an overall QW stack design. Also observed are the ripples characteristic of interference events with the substrate. The depth of the notch for this number of layers and RI contrast is lower than the predicted value (eq 1) due to the finite values of absorption present in each material. Small values greatly reduce the effective reflectivity. Inputs to the design model included the number of layers, the thickness of the layers, and the RI and absorption coefficient as a function of wavelength. Experimental values were extrapolated to incorporate wavelengths into the near-infrared. The positions of the peaks and the magnitude of the notch are close, which is remarkable given the serial nature of the deposition process. This indicates good control over the deposition conditions and indicates that with this technique PECVD of organic precursors can be utilized to deposit optical films with good thickness control.

In general, many PECVD processing parameters can be changed to alter film structure and properties. These parameters include the geometry of the reaction chamber (which affects the flow dynamics); frequency, power,

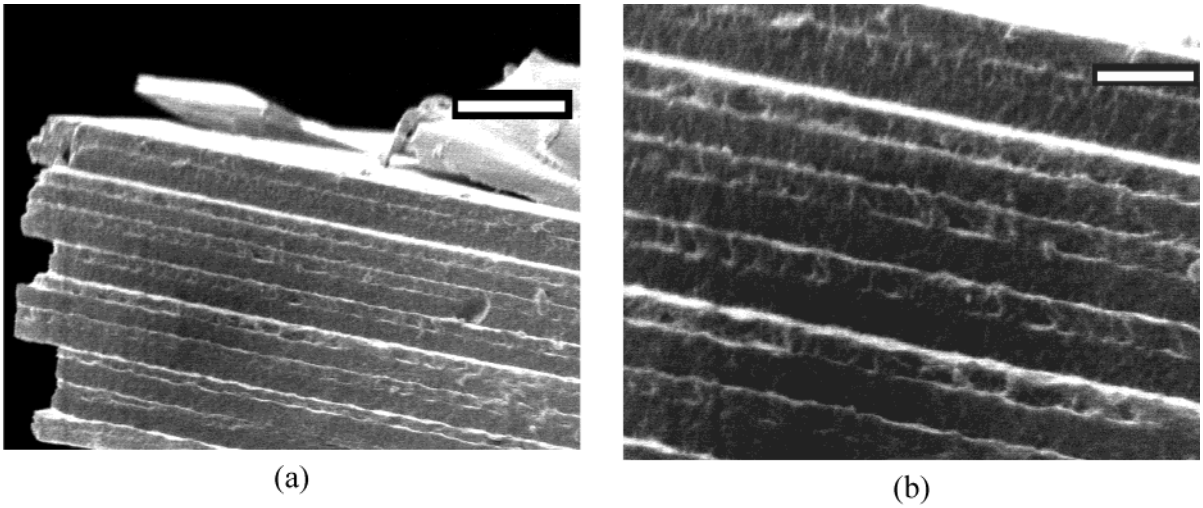

Figure 9. Scanning electron micrographs of the fractured cross-section of the multilayer stack consisting of alternating high and low refractive index films. Scale bars correspond to 1.5 μm and 600 nm.

and type of the RF discharge; shape, type, and location of the substrate; input position and flow rate of precursors; the type of discharge gas; pressure and temperature in the reaction chamber; and different plasma geometries (plate electrodes or coil). This range of processing conditions allows for a great deal of flexibility in the final thickness, morphology, chemical structure, and deposition rate.

The next step using this approach is to demonstrate the feasibility of continuously grading the refractive index between the two extreme values as an approach to achieve nonconventional RI profiles. Modification of the experimental setup to allow continuous monitoring of two simultaneous feed rates has occurred. Work is currently centered on varying the feed position and mass flow rates in an attempt to obtain any refractive index between the extremes.

Acknowledgment. We are much indebted to Dr. Peter Haaland, Mobium Inc., for stimulating suggestion and helpful discussion of PECVD work, and to Prof. Hercules, Vanderbilt University for unpublished TOF-SIMS data which confirmed the PP-benzene cross-linked structure. We also thank Dr. Paul Fleitz and Byron Edmonds of AFRL/MLPJ for their support of this study.

CM0206542